Fluorescent Dye Adsorption in Aqueous Suspension to Produce Tagged Cellulose Nanofibers for Visualization on Paper

Emilia Purington[1], **Douglas Bousfield**[1], and **William M Gramlich**[2,*]

[1]Department of Chemical and Biological Engineering, Paper Surface Science Program, University of Maine, Orono, ME 04469

[2]Department of Chemistry, Paper Surface Science Program, University of Maine, Orono, ME 04469

Abstract

Cellulose nanofibers (CNFs) have great potential to be a layer in packaging materials because of their good barrier properties. When paper is coated with CNFs, they are difficult to distinguish from the base sheet. This issue creates challenges when trying to determine where CNFs migrate relative to the paper fibers during coating and drying. A three- dimensional analysis is possible by using confocal laser scanning microscopy (CLSM) if CNFs can be tagged with fluorescently active groups. In this study, CNFs were fluorescently tagged through adsorption of fluorescent dyes such as fluorescein isothiocyanate (FITC) and thioflavin by mixing with CNFs in their native suspension followed by purification. The adsorbed dye remained attached during typical coating procedures, low pH values, and high ionic strengths, but not for high pH and in contact with acetone. CNFs were also covalently tagged with FITC following methods reported in the literature as a comparison to already established methods for tagging cellulose nanocrystals (CNCs). Images of never dried samples indicated that covalently tagging CNFs altered the state of the fines dispersion, while dye adsorption did not. Coatings of the adsorbed dye tagged CNFs on paper were successfully imaged by CLSM since the concentration of dye in the water phase was low enough to provide a good contrast between regions of CNFs and paper. With this method, the location and potential migration of CNFs coated on paper were successfully determined for the first time to the best of our knowledge. CNF based coatings with solids larger than 2.8% were found to have a distinct layer of CNFs at the paper surface with little CNFs penetrating into the paper structure, but lower solids result in significant penetration into the paper.

Introduction

Cellulose nanofibers (CNFs) are fine scale fibers obtained from the mechanical treatment of wood fibers with high surface area and individual fiber strength (Bhatnagar and Sain, 2005). These unique renewable materials have great potential to produce novel products such as formaldehyde free particle board (Amini *et al.*, 2017), plastic composites, medical devices,

*corresponding author: william.gramlich@maine.edu.

packaging materials (Mousavi *et al.*, 2017), biological membranes (Barhate and Ramakrishna, 2007), and aerosols filters (Munir *et al.*, 2015). Additionally, the biodegradability of CNFs makes them a strong candidate for use in drug delivery and medical device implementation (Dersch *et al.*, 2005).

One key area of interest is to utilize the unique properties of CNFs to create new paper-based materials that can be recycled with paper and are compostable. Paper coatings that are generally comprised of pigments held together by binders like starch and latex are an important aspect of paper-based materials. During the coating and drying processes, these binders are known to migrate within the coating layer, effecting print and barrier qualities (Du *et al.*, 2011). As a result, utilizing different binder components and understanding binder migration has been a research focus (Hagen, 1986). Due to their interesting properties, the use CNFs as a binder within a coating system (Richmond *et al.*, 2014) or as a coating layer itself (Honorato, 2015, Mousavi *et al.*, 2017, Kumar et al. 2017, Mousavi *et al.* 2018) have been investigated. The addition of CNFs to pigments can create super hydrophobic paper (Arbatan *et al.*, 2012) and coated CNFs reinforce paper as well as imparts grease and air resistance for barrier coatings (Aulin *et al.*, 2010). Brodin *et al.* (2014) and Lavoine *et al.* (2012) review the barrier properties of the CNF films. However, in the production of these products, the extent that CNFs migrate into the paper during the application and drying stages is unclear, causing inefficient use and potentially unwanted properties.

Imaging CNFs on paper is challenging due to their high aspect ratio, nanometer diameter, and chemical similarity to the paper fibers. Atomic force microscopy (AFM) can give the morphology and size distribution of the fibers before coating (Bhatnagar and Sain, 2005), but do not give information with regard to CNF migration after coating. Similarly, scanning transmission electron microscopy (STEM) can image the individual fibrils of CNFs (de Morais *et al.*, 2010) and scanning electron microscopy (SEM) yields detailed surface information, including topographical maps of CNF films (Pei *et al.*, 2013). The surface of CNFs on paper substrates have been imaged using SEM (Fantini and Costa, 2009, Kumar *et al.*, 2017); however, CNFs could not be distinguished from the paper fibers. Cross sections of paper coated with CNFs (Ottesen *et al.*, 2017) showed an apparent concentrated layer of CNFs covering the paper fibers, but the extent to which the CNFs migrated into the paper structure was not clear. Using these various imaging methods, the location of CNFs has been challenging to distinguish from that of the paper fibers when used in paper coatings. Moreover, these microscopy techniques give local information, but have difficulty imaging over larger length scales. Light-based imaging techniques can give longer range information and consequently paper coatings have been imaged with confocal laser scanning microscopy (CLSM) and fluorescence microscopy (FM) to determine the location of binders (Purington *et al.*, 2017). However, these imaging techniques require that the samples imaged are fluorescently active, necessitating tagging CNFs with fluorescent molecules to implement these techniques.

To fluorescently tag CNFs, work has focused on covalently attaching fluorescent dyes to the CNF surface. Tagging has been conducted in organic solvents through carbazole (Karakawa *et al.* 2007) and amine (Yang and Pan, 2010) functionalizations; however, solvent exchange methods have the potential to change the nature of CNFs due to various interactions. As a

result, functionalization with dyes under native conditions (i.e. water suspension) has been a focus of research. Acid-alkali treatment of rice husks prior to mechanical treatment (Kalita *et al.*, 2015) has produced fluorescent phenylcoumarone groups from lignin. More often CNFs and other cellulose nanomaterials have been functionalized in water after fabrication. One method has been to use chloro-substituted triazine ring functionalized dyes to react with the hydroxyl groups of CNFs and cellulose nanocrystals (Zanmorano *et al.* 2011, Grate *et al.*, 2015). Another method has been to introduce amines to the cellulose surface in water. Cellulose nanocrystals (CNCs) have been tagged through a three-step functionalization process, which consists of epoxy functionalization, amine modification, and then coupling the amine to fluorescein isothiocyanate (FITC) (Dong *et al.*, 2007), rhodamine B isothiocyanate (RBITC) (Mahmoud *et al.*, 2010), or a pyrene based dye (Zhang *et al.*, 2012). This system has been modified to create a one pot series of reactions with both FITC and RBITC (Nielsen *et al.*, 2010). These modifications also have recently been successful in tagging CNFs with RBITC (Ding *et al.*, 2018) for use in paper applications. These tagging procedures chemically modify the cellulose surface and although often low levels of modification are targeted, they can alter the surface chemistry and subsequent CNF behavior as compared to the native CNFs. Less intrusive methods to tag CNFs are needed to ensure accurate imaging and CNF behavior.

A potential non-destructive way to tag CNFs with fluorescent dye is adsorption. Paper and regenerated cellulose have had a long history of being dyed through adsorption by soaking these materials in solvents containing dyes like Sky Blue FF (Neale and Stringfellow, 1933), benzopurpurine 4B (Hanson and Neale, 1934), chrysophenine G (Willis *et al.*, 1945), Direct Blue 15 (Nango *et al.*, 1984), and others (Maekawa *et al.*, 1989, Agnihorti *et al.*, 1972, Bae *et al.*, 1996). Though dry cellulose can successfully adsorb a wide range of dyes once placed in a solvent, pulp, CNFs, and CNCs are already dispersed in the solvent, potentially complicating adsorption. By amino-functionalizing of CNCs to create surface positive charges, Jin *et al.* (2015) adsorbed various anionic dyes through electrostatic attraction in aqueous solutions, overcoming some of these challenges, but still requiring potentially material altering reactions. A recent report indicates that Congo red can be added directly to CNFs, tagging through adsorption and suggesting that other dyes may do the same (Wang *et al.*, 2018).

Several mechanisms for dye adsorption to cellulose have been proposed and measured for aromatic dyes like those that show fluorescent activity. Congo red adsorption has been attributed to the electrostatic interactions between hydroxyls of the cellulose and the polar groups of the dye (Pérez and Mazeau, 2005). Similarly, both Congo red and calcofluor (Wood 1980) have adsorbed to a greater extent on more functionalized polysaccharides which is consistent with an electrostatic effect. Methylene blue can adsorb to CNCs through a heterogeneous chemisorption mechanism where a monolayer of the dye coated fibrous surfaces in a hydrogel (Zhou *et al.*, 2014). Carbohydrate-aromatic (CA) interactions from van der Waals forces (CH-π interactions) and the hydrophobic effect also have been reported to explain adsorption of aromatic molecules to carbohydrates such as cellulose in aqueous environments (Chen *et al.*, 2013, Asenio *et al.*, 2012). These CA interactions as opposed to electrostatic interactions likely account for most of the observed binding in aqueous systems (Chen *et al.*, 2013). The most notable example of observed CA interactions has been the

adsorption of aromatic residues to cellulose in the cellulose binding domains of proteins (Linder and Teeri, 1997, Georgelis *et al.*, 2012). Since electrostatic interactions, van der Waals forces, and hydrophobic effects have all been reported to affect aromatic molecule adsorption to cellulose or similar molecules, likely all these could affect dye adsorption, requiring individual investigation of each dye desired for tagging.

Since the structure of FITC is similar to previously adsorbed molecules, we hypothesized that FITC would adsorb to CNFs, tagging them for CLSM imaging. In this study, FITC was adsorbed to CNFs and compared to a model FITC reacted CNFs using the three-step functionalization process described by Ding *et al.* (2018). Adsorption of other common dyes to CNFs and their adsorption stability also were characterized. Dye adsorbed tagged CNFs were coated on paper and the penetration depth was measured, demonstrating the utility of these tagging methods to track CNFs in paper and determining the relationship between CNF solids content and coating penetration. To the best of our knowledge, this is the first time that CLSM has been used to track the location of CNFs when coated on paper. Furthermore, dye was not observed throughout the entire paper after coating, which indicates that the adsorbed dye was stable on the CNF surface and at a low concentration in the water phase.

Materials and Methods

Materials

The CNFs used had a total solids content of 3.7 wt% made from softwood bleached Kraft pulp and was obtained from the University of Maine Process Development Center. To determine an average fibril diameter, the CNFs were diluted to 0.04 wt% using DI water and evaporated on copper grids using uranyl acetate as a negative contrast agent. The grid sample was imaged by transmission electron microscopy (TEM) (CM10, Philips) to characterize the CNFs in terms of average fiber diameter. Images were collected with the Gatan Microscopy software (v2.31) and analyzed using ImageJ software (v1.48). For each TEM image, a 4×4 grid was inserted using ImageJ and the diameter of every fiber that intersected the grid was determined. The average fiber diameter of the CNFs was determined to be 124 ± 25 nm.

Rhodamine B used for the tagging was purchased from Wako Chemicals. Acridine orange, fluorescein isothiocyanate (FITC), Nile blue, and thioflavin dyes used for the fluorescent tagging were purchased from Sigma Aldrich. The epichlorohydrin (ECH), sodium hydroxide (NaOH), ammonium hydroxide (NH_4OH), sodium chloride (NaCl), sodium borate, acetone, and sulfuric acid were purchased from Fisher Scientific and used without further purification. Newsprint was from an industrial source and used for all coatings as it represents a medium thickness paper that is highly absorbent, containing ground wood fibers.

Adsorption of fluorescent dyes to CNFs

Various fluorescent dyes were added to CNFs to investigate the adsorption of the dyes on CNFs. For each dye, 0.05 g of dye (between 1.1 and 1.5 mmol dye per gram of CNFs) was

added to 50 mL of DI water and stirred for half an hour to disperse completely. Simultaneously, 20 mL of DI water was added to 30 mL of 3.7 wt% CNFs and allowed to stir for half an hour. The pH of the CNF suspension was near neutral and was not adjusted at this point. The dye water was then added to the CNFs and stirred in the dark for two hours at room temperature. After two hours, the CNFs were centrifuged at 7000 RPM and washed with excess DI water until the decant water was clear and free of color. Aliquots of the CNFs after purification were taken for UV-Vis analysis (Figure S1)

Functionalization of CNFs with FITC

A modified literature procedure was used to covalently functionalize CNFs with FITC (Ding *et al.*, 2018) and is shown in Figure 1. In an example procedure, epoxy groups were functionalized off the hydroxyl groups by reacting 15 mL of 3.7 wt% CNFs with 250 μL of ECH in the presence of 50 mL of 1.34M NaOH for 2 h at 60 °C. Unreacted reagents were removed by centrifugation operating at 7000 RPM and washing with excess DI water five times. To introduce the amine groups, the purified CNFs were brought to pH 12 with 1.34 M NaOH and reacted with 2.8 mL of NH_4OH for 2 h at 60 °C. Afterwards, further centrifugation at 7000 RPM and washing was done five times to remove unreacted reagents. At this point, 0.07 g FITC was added to 50 mL DI water and stirred to fully disperse for half an hour. Simultaneously, 1.05 g NaCl and 2.3 g sodium borate were added directly to the CNFs and stirred for half an hour. The FITC water was added to the CNFs and stirred overnight at room temperature in the dark to functionalize the CNFs with FITC. The reaction mixture was then centrifuged at 7000 RPM and washed with excess water until the decanted water was clear and free of yellow color. Aliquots of the CNFs after purification were taken for UV Vis analysis.

Evaluations of adsorbed dye stability

Organic solvent stability.—To examine organic solvent stability of the FITC adsorption, 10 mL of the FITC adsorbed CNFs were added into 200 mL acetone and stirred for two hours. The acetone and CNFs were centrifuged at 1550 RPM and washed with excess DI water three times. After the washes, the pH of the CNFs was neutralized back to 7 using HCl. Aliquots of the CNFs were prepped for UV-Vis analysis.

pH stability.—To examine the stability of adsorbed FITC to pH changes, FITC adsorbed CNFs were exposed to different pH values. Hydrochloric acid was added to adjust 5 mL of FITC adsorbed CNFs to acidic pH values of 1.5, 2, 3, and 3.5, separately, while NH_4OH was used to achieve pH values of 10, 11, and 12, separately. Upon addition of the acid or base, the CNFs were stirred for five minutes. After five minutes, the samples were left for half an hour before they were centrifuged and washed with excess DI water three times. After the washing, the remaining CNFs were neutralized to pH 7 and aliquots of the FITC adsorbed CNFs were prepped for UV-Vis analysis.

Salt stability.—To examine the stability of adsorbed FITC to salt solutions, FITC adsorbed CNFs were washed with concentrated brine water. For this test, 10 mL of the FITC adsorbed CNFs were mixed with 200 mL of 1M NaCl water and stirred for two hours. The CNFs in

brine water were centrifuged at 1550 RPM and washed with excess DI water three times. The washed CNFs were collected and analyzed with UV-Vis spectroscopy.

UV-Vis Analysis

To find the molar ratio of dye to repeat unit (F/C) for the tagged CNFs by UV-Vis spectroscopy, the CNFs were first degraded with cellulase from *Trichoderma reesei* (Sigma Aldrich). Approximately 1 mL of CNFs (between 0.01 and 0.02 g dry weight) was lyophilized and sodium acetate buffer (pH 5) was added to the dry CNFs to make a 1 wt% suspension. For every 1 mL of buffer used, 10 μL of enzyme was added, the sample was vortex mixed for a few seconds, and then placed into an incubator at 50 °C overnight (18 h). The next day, 5 μL of enzyme was added to the sample and placed into the incubator for another 2 h. The degraded CNF samples were placed in the UV-Vis spectrometer (Beckman DU 7500) for analysis with an air background. The step size for the data analysis was set to 1 nm and the sample absorbance was scanned from 350 to 650 nm. Using the absorbance obtained from UV Vis spectroscopy, the concentration of dye was calculated using Beer's Law as

$$C = \frac{A}{\varepsilon l}$$

where C is the concentration of dye, A is the measured absorbance, ε is the measured molar absorptivity and l is the path length of the cuvette. Using a calibration curve, the molar absorptivity for each dye studied were determined to be 216600, 13600, 4700, 59400, and 9800 M^{-1} cm^{-1} for FITC, acridine orange, Nile blue, rhodamine B, and thioflavin, respectively, in sodium acetate buffer at pH 5 (Figures S2–S6). The number of moles of dye (n) was calculated from the concentration of dye (C) using the known volume analyzed. The ratio of dye molecules to CNF anhydroglucose repeat unit was calculated to find the degree of functionalization, using the molecular weight of anhydroglucose (162.2 g/mol) and the dry mass of the CNFs.

Blade Draw Down Coatings Method

A blade draw down coating method was used to coat paper with the tagged CNFs. To coat paper, paper strips (4 by 28 cm) were taped down to a 30 cm by 30 cm piece of tempered glass with a plastic sheet (Mylar, Dupont) covering the top 2 cm of the paper strip. Approximately 3 mL of CNF suspension was poured onto the plastic. The blade draw down coater was placed on the plastic sheet above the wet coating components and drawn down in a swift, even motion to the end of the paper by hand. The coatings were placed into an oven at 105 °C for 20 min to dry.

CLSM Procedures

Physical cross sections of coating samples were made by cutting thin slices of the samples, usually about 1 mm by 2 cm long, and placing them sideways in between two coverslips for imaging. The samples were imaged by a confocal laser scanning microscope (TCS SP2, Leica). The pinhole size was automatically adjusted for the best imaging and ranged from 60 to 80 μm. The excitation, emission acceptance, and reflected light acceptance wavelengths

for the various dyes used are shown in Table 1 below. Reflected light was collected by collecting the emissions from a 10 nm range while exciting the samples with laser within that range. Each sample was excited with the laser and scanned. Each sample was scanned between 40 to 50 μm in the z direction for ten scans. The fifth scan in the series was used for the imaging analysis as to avoid edge effects during the sample preparation. Images were collected with the Leica Confocal software (v2.61) and merged and analyzed using ImageJ software (v1.48).

Results and Discussion

Quantification of Tagging

Since CNFs have high surface area (Sehaqui *et al.*, 2011), we hypothesized that they had thepotential to adsorb different types of dye molecules. The FITC adsorbed CNFs were visiblyyellow after washing (Figure S7). The cellulase degraded CNF samples were analyzed usingUV-Vis spectroscopy to quantify dye adsorption at 485 nm (Figure S8), consistent withFITC. The amounts of FITC on CNFs after the reaction procedure and after adsorption were0.32 and 0.04 mmol FITC per mole of CNF glucose repeat unit (F/C), respectively, as shownin Figure 2. The reacted samples had ten times the amount of FITC compared to the simpleadsorption, but the amount of dye firmly attached to CNFs was not clear.

Figure 2 also shows the degree of functionalization for the reacted material after precipitation with acetone, the adsorbed sample after precipitation with acetone, and an adsorbed FITC sample washed with brine (1 M NaCl). The decrease in F/C of the reacted CNFs after precipitation shows that a large amount of FITC was loosely attached to the CNFs and comes off the fibers to some extent after contact with acetone; only 8% of the initial amount remains (Figure S9). This result is interesting as it suggests that the previously reported functionalization reactions likely made the CNFs more amenable to adsorption rather than covalently attaching all fluorescent molecules much like the reported amine functionalization improving adsorption to CNCs (Jin *et al.* 2015). The FITC was only covalently attached at 2.5×10^{-2} F/C value after the acetone precipitation, which is comparable to the original FITC on the FITC adsorbed CNFs. The adsorbed CNFs had a significant amount of dye, but after contact with acetone, no FITC was detected. The brine solution did not influence FITC amount, which indicates that the adsorbed CNFs were not influenced by ionic strength at this pH.

To further understand the adsorption of the FITC on the CNF and its stability, the FITC adsorbed CNFs were exposed to aqueous solutions with different pH values by adding acid or base to the CNFs. FITC has several acidic protons with different pK_a values so if the adsorption phenomenon was due to electrostatic interactions, the adsorbed FITC was hypothesized to be unstable when the pH was changed. Once the FITC adsorbed CNFs were adjusted to non-neutral pH values, it was centrifuged to remove water that had visible FITC. The CNFs were then neutralized back to pH 7, degraded, and analyzed with UV Vis spectroscopy to measure the amount of remaining FITC on CNFs. From UV Vis spectroscopy data given in Figure 3, the acidic treated CNF suspension still showed signal from FITC while the basic treated CNFs did not. Compared to the original FITC adsorbed

CNFs, the acidic treated CNFs had between 20 and 60% of the FITC remaining while the basic conditions had less than 2%. These results suggest that pH can play a role in controlling the adsorption of FITC to CNFs. At high pH values (pH > 7.4) (Lorenz and Gruenstein, 1999), the FITC molecule should be fully deprotonated, resulting in a doubly negatively charged molecule and increased water solubility, which may cause it to desorb. At pH values below 7, the FITC has three pK_a values, which indicates that it transitions between negatively charged, neutral, and positively charged (Smith and Pretorius 2002). Below a pH of 4, the FITC should be nearly fully protonated (i.e. neutral charge) and thus less soluble in water and unlikely to desorb from the CNFs. As the pH decreases, the FITC becomes positively charged (pK_a ca. 2.3) and likely more water soluble. This increased solubility at very low pH values could describe the observed decrease in F/C as the pH is decreased. The decrease in F/C at low pH also may be caused by some hydrolysis of the cellulose surface that would led to the detachment of dye.

To explore dye functional groups or properties that influence dye adsorption to CNFs, the adsorption of several chemically different fluorescent dyes (Table 2) was studied (Figure S10 and S11). These molecules have different pK_a values, polarities, and molecular sizes that could affect their adsorption to CNFs. Each dye was dispersed in water for half an hour, added to the CNFs, and stirred for another two hours, mimicking the adsorbed FITC CNF method. Dye adsorbed CNFs were centrifuged and washed with excess DI water about 25 times for the acridine orange, rhodamine B, and thioflavin CNF samples, and 50 times for the Nile blue CNF sample. After the centrifugation and washing, the supernatant from the acridine orange, rhodamine B, and thioflavin treated CNF samples were clear and free of color. The supernatant from the Nile blue CNFs was still tinted blue, but to a substantially lower degree than originally. Aliquots of dye adsorbed CNFs were degraded and analyzed using UV Vis spectroscopy. When compared to the adsorbed FITC CNFs (3.9×10^{-2} F/C), more Nile blue, acridine orange, and thioflavin adsorbed to the CNFs, while less rhodamine B adsorbed (Table 2). Furthermore, the acridine orange was stable on the CNFs under both acidic and basic conditions (Figure S12), while the thioflavin was not stable after pH treatments (Figure S12). Additionally, these results outline one of the benefits of using adsorption to fluorescently tag CNFs as different dyes can be used without the need of reactive groups, providing flexibility for the target application.

To connect the chemical properties of the different dyes to their propensity for adsorption, a couple of parameters were considered as summarized in Table 2. CNFs are typically negatively charged due to some carboxyl groups remaining from hemicelluloses, enabling positive charged compounds to adsorb to its surface (Ahola *et al.* 2008). Such an effect was observed, as the positively charged dyes at pH 7 (i.e. acridine orange, Nile blue, and thioflavin) adsorbed to the greatest extent (Table 2). According to previous studies, the anionic groups of the CNFs could create binding sites for the dimers of acridine orange and thioflavin on the CNFs (Houtman et al., 2016), which can explain the 100-fold increase in acridine orange and thioflavin adsorption over the other dyes. In addition, cationic dyes like acridine orange and thioflavin have an affinity to stain the lignin present within the CNFs (Drnovsek and Perdih, 2006). While little lignin is present in the CNFs (0.3%) as compared to hemicellulose (16.4%), this small amount of lignin could contribute to the higher F/C values due to the high binding affinity. Rhodamine B exists as a zwitterion at neutral pH,

which limits its solubility in water and resulted in limited adsorption. However, negatively charged FITC adsorbed significantly, which would not be expected if electrostatic interactions were the only driving force for adsorption, suggesting that molecular charge was not the only parameter that affected adsorption. The topological polar surface area (tPSA) is the sum of the polar surfaces of a molecule and has been related to drug adsorption processes (Ertl *et al.* 2000). The three compounds that adsorbed to the greatest extent, acridine orange, Nile blue, and thioflavin, have the lowest tPSA values (Table 2), indicating that they are relatively hydrophobic. Cellulose has hydrophobic faces due to the hydroxyl groups being axial in the cellobiose repeat unit where these dyes can adsorb through the hydrophobic effect (Matthews *et al.* 2006) and be stabilized by CA interactions. FITC adsorption is likely governed by this hydrophobic affect and CA stabilization as well rather than electrostatic interactions, but due to its more polar structure, it does not adsorb to the same extent as the less polar dyes.

CLSM imaging

With the CNFs successfully tagged with FITC using both covalently linked and adsorbed methods, its utility to quantify migration into paper was investigated. The FITC tagged CNF suspensions were imaged, which yielded fluorescence activity for reacted and pH 1.5 treated adsorbed FITC samples. All FITC adsorbed CNFs that were pH treated after adsorption showed fluorescence activity, so a suspension treated at a pH of 1.5 was chosen as representative pH treated CNFs (Figure S13). This treated FITC adsorbed CNF suspension was used for subsequent imaging.

The images in Figure 4 from FITC reacted CNFs are quite different than those for the adsorbed FITC CNFs. For FITC reacted CNFs, fluorescent micrometer-scale fibers are visible against a black background, while the images from the adsorbed FITC CNFs show continuous fluorescence. This result suggests that the covalently labeled CNFs have a structure that is different than the native CNFs. This contrast between the FITC reacted and adsorbed CNFs may be due to the reactions performed making the fines to be flocculated into fiber like structures or removed during the purification steps. The fine fibers of the FITC reacted CNFs appeared to be more dispersed in water as evidenced by the colored aqueous layer above the bulk CNF suspension before purification. This dispersed layer of fines was decanted off the bulk CNF suspension after centrifugation, leaving behind the larger fibrils. For the adsorbed FITC CNFs, the CNF fines were not removed during centrifugation and were still intertwined between the larger fibrils, creating a continuous region of fluorescence. From TEM imaging and characterization of the fibrils, the average fibril diameters for the FITC reacted and FITC adsorbed CNFs were 150 ± 40 (Figure S14) and 120 ± 50 nm (Figure S15), respectively. The FITC adsorbed CNFs are close to the original CNF diameter of 120 ± 30 nm (Figure S16). From this characterization and the images of Fig. 4, the reacted CNF samples still have fine fibers, but they are floculated into fiber like structures that are on the order of a few micrometers in diameter. However, when the CNF samples were lyophilized (freeze dried), all the CNF samples showed micrometer-scale fiber structures in the images (Figure 4 and S17). Freeze drying CNFs is known to induce irreversible hydrogen bonding, causing the fines to concentrate into fiber structures (Han *et al.*, 2013). Though the fine structure of CNFs was lost upon drying, these results confirmed

that FITC tagged CNFs can be dried and used for imaging and that the adsorbed FITC CNFs are sufficiently tagged for imaging.

Both FITC reacted CNFs and adsorbed FITC CNFs were coated on newsprint at about 2 wt % solids and 10 grams per square meter (gsm) to observe how the tagged CNF preparation method affected microscopy results. In the 2D CLSM images (Figure 5A), less fluorescence is seen in the adsorbed CNFs than in the reacted CNFs at the surface of the paper. The difference in the amount of fluorescence between the adsorbed and reacted CNFs corresponds to the results in Figure 2 and the images of Figure 4 that show an increase in fluorescence and a fiber structure for the reacted CNFs. In the dry coating layer, the fine fibrils of the adsorbed CNFs define and outline the fibrous structure of the base paper while the larger fibrils of the reacted CNFs cover the paper fibers. The retained fines in the adsorbed CNFs are more mobile than the large fibrils of the reacted CNFs, which may lead to them coating the paper fibers as seen in Figure 5. Though the top down images of the FITC signals in Figure 5 show some differences, these images of the adsorbed and reacted CNFs show the same outlines of paper fiber structures at the surface of the paper with the reacted CNFs providing greater fluorescence signal. Similarly, the cross section CLSM images of both the FITC reacted and adsorbed CNF samples (Figure 5B) show that most of the CNFs are at the surface of the paper with moderate penetration into the base paper in some locations. Even though the adsorbed CNFs maintains the fines post purification, the cross sectional CLSM images are like that of the reacted CNFs, which does not maintain the fines. The comparable results of the CLSM images of the adsorbed CNFs to the reacted CNFs provides a tool to further understand how CNFs behaves as a coating layer.

Similar to the FITC adsorbed CNFs, the other dye adsorbed CNFs were also coated on newspaper at 1.5% wt solids and imaged with the CLSM. As seen in the CLSM images (Figure 6), each of the dyed CNFs showed signal upon imaging, regardless of the amount of dye adsorbed to the CNFs. For the Nile blue and rhodamine B samples, the CNFs appear to be penetrating through the entirety of the paper substrate, which is likely due to some free dye in the water phase. The Nile blue CNF wash waters during purification were still tinted blue after 50 washes, which suggests that the dye desorbs to some extent upon contact with DI water. Some Nile blue particles settled to the bottom of the CNF suspension after centrifugation, most likely due to a low solubility in water and a large excess of dye added initially. The rhodamine B CNFs, on the other hand, showed rhodamine B at the bottom of the CNF suspension in the centrifuged samples, with no visible color in the CNFs or the supernatant, suggesting that the rhodamine B did not adsorb to the CNFs. Acridine orange and thioflavin adsorbed CNFs produced results similar to the FITC adsorbed CNFs results, demonstrating that they also can be used reliably to determine the location of CNFs on paper.

With these new tools to observe how CNF solids content affects CNF penetration into an absorbent substrate, coatings were made using different wt% (1, 2, 2.8 and 3.5) of FITC adsorbed CNFs on newsprint and imaged with CLSM (Figure 7). A higher solids content coating of 4.3 wt% was attempted; however, the CNFs clumped up and did not form a uniform coating (Figure S18). Additionally, the thickness of the newsprint and coating layer (from the reflected light channel) and the coating signal (from the FITC channel) were

measured using five evenly spaced areas from the top to the bottom of the CLSM image as reported in Table 3. Overall, the higher the solids content of the CNF coatings, the thicker the paper appears in the CLSM images due to the CNFs sitting on top of the base paper. The lowest solids content CNF coatings penetrated the furthest into the base paper with CNF signal showing *circa* 80% penetration of the CNFs into the base paper for 1 and 2 wt% CNF solids, based on an average CLSM paper thickness of 52 ± 6 μm. At 2.8 wt% there is less penetration into the base paper (20%) while the 3.5 wt% solids coating seems to sit on top of the paper (only 9% penetration into the base paper) with a uniform coating layer. Even though the 3.5 wt% solids seemed to start to have issues with the application of the coating where the CNFs clump up and is difficult to coat, the coating layer in CLSM images seems to relatively uniform; however, this is a small representation of the whole coating. In this study, coatings with 2.8 wt% CNF solids and higher do not significantly penetrate an absorbent base paper as seen by the increase in the paper and coating thickness. As the solids content is increased, there is less water present in the same volume that can potentially pull the CNFs into the absorbent base paper. Additionally, the higher solids content increases CNF viscosity and causes entanglement of the CNFs which leads to the fibrils jamming at the paper surface and resulting in less CNF penetration. These results agree with Mousavi et al. (2018) and Ottesen *et al.* (2017) that obtained an apparent CNF layer at similar solids levels. As a result, more of the CNFs are present at the paper coating surface, creating a more uniform coating layer. At these high solids, excess water exists that penetrates into the paper, which should bring non-adsorbed dye deeper into the sheet that should be observed throughout the paper during imaging. Since no dye was found deep inside the paper structure at high solids, little dye was left in the water layer, which confirms most of the dye was adsorbed to CNFs.

Conclusions

Straightforward methods were developed to tag CNFs with fluorescent dyes through physical adsorption that were stable under various conditions and yielded CLSM images comparable to that of reactively coupled FITC CNFs. While FITC dye was used to successfully fluorescently tagged through covalently binding and physical abortion to the CNFs, physical adsorption was found to not be unique to FITC as other aromatic dyes were observed to adsorb through positive electrostatic interactions, the hydrophobic effect, and aromatic-carbohydrate interactions, indicating that other small, positively charged aromatic dyes and compounds should adsorb to CNFs. Specifically, acridine orange and thioflavin were found to adsorb on CNFs to a significant and stable level. This adsorption phenomenon provided an easy method to image its location using fluorescence microscopy that proved useful for CNF paper coatings. As the solids content of the CNFs was increased, the CNF penetration into the base paper decreased. At 2.8 wt% solids, CNFs no longer penetrated significantly into newsprint, forming a continuous film upon the paper surface. Furthermore, adsorbed dye remained with the CNFs, which demonstrated that little dye was free in the water phase and enabling this CLSM imaging and measurements. By developing a technique for fluorescently tagging CNFs, the CNFs can be distinguished from the paper and the migration of the CNFs can be studied in future work.

Supplementary Material

Refer to Web version on PubMed Central for supplementary material.

Acknowledgments

References

Agnihotri VG, & Giles CH (1972). The cellulose–dye adsorption process. A study by the monolayer method. Journal of the Chemical Society, Perkin Transactions 2, (15), 2241–2246.

Ahola S, Österberg M, & Laine J (2008). Cellulose nanofibrils—adsorption with poly(amideamine) epichlorohydrin studied by QCM-D and application as a paper strength additive. Cellulose, 15:303–314.

Amini E, Tajvidi M, Gardner DJ and Bousfield DW, (2017). Utilization of cellulose nanofibrils as a binder for particleboard manufacture, Bioresources 12(2): 4093–4110

Arbatan T, Zhang L, Fang XY, & Shen W (2012). Cellulose nanofibers as binder for fabrication of superhydrophobic paper. Chemical engineering journal, 210, 74–79.

Aseno JL, Arda A, Canada FJ, & Jimenez-Barbero J (2012). Carbohydrate–aromatic interactions. Accounts of chemical research, 46(4), 946–954. [PubMed: 22704792]

Aulin C, Gällstedt M, & Lindström T (2010). Oxygen and oil barrier properties of micro fibrillated cellulose films and coatings. Cellulose, 17(3), 559–574.

Bae SH, Motomura H, & Morita Z (1997). Diffusion/adsorption behaviour of reactive dyes in cellulose. Dyes and pigments, 34(4), 321–340.

Barhate RS, & Ramakrishna S (2007). Nanofibrous filtering media: filtration problems and solutions from tiny materials. Journal of membrane science, 296(1), 1–8.

Bhatnagar A, & Sain M (2005). Processing of cellulose nanofiber-reinforced composites. Journal of Reinforced Plastics and Composites, 24(12), 1259–1268.

Brodin FW, Gregersen OW and Syverud K, 2014 Cellulose nanofibrils: Challenges and possibilities as a paper additive or coating material–A review. Nord Pulp Pap Res J, 29(1), pp.156–166.

Chen W, Enck S, Price JL, Powers DL, Powers ET, Wong CH, … & Kelly JW (2013). Structural and energetic basis of carbohydrate–aromatic packing interactions in proteins. Journal of the American Chemical Society, 135(26), 9877–9884.Davis, B. W., [PubMed: 23742246]

de Morais Teixeira E, Corrêa AC, Manzoli A, de Lima Leite F, de Oliveira CR, & Mattoso LHC (2010). Cellulose nanofibers from white and naturally colored cotton fibers. Cellulose, 17(3), 595–606

Dersch R, Steinhart M, Boudriot U, Greiner A, & Wendorff JH (2005). Nanoprocessing of polymers: applications in medicine, sensors, catalysis, photonics. Polymers for Advanced Technologies, 16(2-3), 276–282.

Ding Q, Zeng J, Wang B, Gao W, Chen K, Yuan Z, & Tang D (2018). Effect of retention rate of fluorescent cellulose nanofibrils on paper properties and structure. Carbohydrate Polymers.

Dong Shuping, and Roman Maren. Fluorescently labeled cellulose nanocrystals for bioimaging applications. Journal of the American Chemical Society 12945 (2007): 13810–13811. [PubMed: 17949004]

Drnovsek T, & Perdih A (2005). Selective staining as a tool for wood fibre characterization. Dyes and Pigments, 67(3), 197–206.

Du Y, Zang YH and Du J, 2011 Effects of starch on latex migration and on paper coating properties. Industrial & Engineering Chemistry Research, 50(16), pp.9781–9786.

Ertl P, Rohde B, & Selzer P (2000). Fast Calculation of Molecular Polar Surface Area as a Sum of Fragment–Based Contributions and Its Application to the Prediction of Drug Transport Properties. Journal of Medicinal Chemistry, 43, 3714–3717. [PubMed: 11020286]

Fantini D, & Costa L (2009). Dye, fluorophores and pigment coloration of nanofibers produced by electrospinning. Polymers for Advanced Technologies, 20(2), 111–121.

Georgelis N, Yennawar NH, & Cosgrove DJ (2012). Structural basis for entropy-driven cellulose binding by a type-A cellulose-binding module (CBM) and bacterial expansin. Proceedings of the National Academy of Sciences, 109(37), 14830–14835.

Grate JW, Mo KF, Shin Y, Vasdekis A, Warner MG, Kelly RT, … & Wilkins MJ (2015). Alexa fluor-labeled fluorescent cellulose nanocrystals for bioimaging solid cellulose in spatially structured microenvironments. Bioconjugate chemistry, 26(3), 593–601. [PubMed: 25730280]

Hagen Kenneth G. "A fundamental assessment of the effect of drying on coating quality." Tappi journal 691 (1986): 93–96.

Han J, Zhou C, Wu Y, Liu F, & Wu Q (2013). Self-assembling behavior of cellulose nanoparticles during freeze-drying: effect of suspension concentration, particle size, crystal structure, and surface charge. Biomacromolecules, 14(5), 1529–1540. [PubMed: 23544667]

Hanson J, & Neale SM (1934). The absorption of dyestuffs by cellulose. Part III. A comparison of the absorption of benzopurpurine 4B with that of Sky Blue FF. Transactions of the Faraday Society, 30, 386–394.

Ho N, Weissleder R, Tung C-H (2006). Development of water-soluble far-red fluorogenic dyes for enzyme sensing. Tetrahedron, 62, 578–585.

Honorato Camila, et al. "Transparent nanocellulose-pigment composite films." Journal of materials science 5022 (2015): 7343–7352.

Houtman CJ, Kitin P, Houtman JC, Hammel KE, & Hunt CG (2016). Acridine Orange Indicates Early Oxidation of Wood Cell Walls by Fungi. Plos One, 11(7).

Jin L, Li W, Xu Q, & Sun Q (2015). Amino-functionalized nanocrystalline cellulose as an adsorbent for anionic dyes. Cellulose, 22(4), 2443–2456.

Kalita E, Nath BK, Deb P, Agan F, Islam MR, & Saikia K (2015). High quality fluorescent cellulose nanofibers from endemic rice husk: isolation and characterization. Carbohydrate polymers, 122, 308–313. [PubMed: 25817673]

Karakawa M, Chikamatsu M, Nakamoto C, Maeda Y, Kubota S, & Yase K (2007). Organic Light-Emitting Diode Application of Fluorescent Cellulose as a Natural Polymer. Macromolecular Chemistry and Physics, 208(18), 2000–2006.

Kumar V, Koppolu VR, Bousfield D and Toivakka M (2017). Substrate role in coating of microfibrillated cellulose suspensions. Cellulose, 24(3), pp.1247–1260.

Lavoine N, Desloges I, Dufresne A and Bras J, 2012 Microfibrillated cellulose–Its barrier properties and applications in cellulosic materials: A review. Carbohydrate polymers, 90(2), pp.735–764. [PubMed: 22839998]

Linder M, & Teeri TT (1997). The roles and function of cellulose-binding domains. Journal of biotechnology, 57(1–3), 15–28.

Lorenz JN, & Gruenstein E (1999). A simple, nonradioactive method for evaluating single-nephron filtration rate using FITC-inulin. American Journal of Physiology-Renal Physiology, 276(1), F172–F177.

Maekawa M, Udaka M, Sasaki M, Tujii Y, Yoshida H, Kataoka T, & Nango M (1989). Diffusion mechanism of direct dyes into a cellulose membrane: the structural effect of direct dyes on the adsorption rate. Journal of applied polymer science, 37(8), 2141–2152.

Mahmoud KA, Mena JA, Male KB, Hrapovic S, Kamen A, & Luong JH (2010). Effect of surface charge on the cellular uptake and cytotoxicity of fluorescent labeled cellulose nanocrystals. ACS applied materials & interfaces, 2(10), 2924–2932. [PubMed: 20919683]

Matthews JF, Skopec CE, Mason PE, Zuccato P, Torget RW, Sugiyama J, Himmel ME Brady JW (2006). omputer simulation studies of microcrystalline cellulose Iβ. Carbohydrate Research, 341, 138–152. [PubMed: 16297893]

Mousavi SM, Afra E, Tajvidi M, Bousfield DW, & Dehghani-Firouzabadi M (2017). Cellulose nanofiber/carboxymethyl cellulose blends as an efficient coating to improve the structure and barrier properties of paperboard. Cellulose, 24(7), 3001–3014.

Mousavi SM, Afra E, Tajvidi M, Bousfied DW, and Dehghani-Firouzabadi M (2018). Application of cellulose nanofibril (CNF) as coating on paperboard at moderate solids content and high coating speed using blade coater. Progress in Organic Coatings, 122, 207–218.

Munir MM, Abidin MS, & Rajak A (2015). A Computer-Based Air Flow Control System for Aerosol and Filtration Research In Applied Mechanics and Materials (Vol. 771, pp. 137–140). Trans Tech Publications.

Murad MM (1999). Fluorescence analysis of acridine orange adsorbate at the water/N- heptane interface, bulk and interface. Journal of Fluorescence, 9(3), 257–263.

Nango M, Maekawa M, Katayama A, & Kuroki N (1980). Dyeing of cellulose by direct dye in aqueous sodium alginate solution. Journal of Applied Polymer Science, 25(10), 2159–2166.

Neale SM, & Stringfellow WA (1933). The absorption of dyestuffs by cellulose. Part I.— The kinetics of the absorption of Sky Blue FF on viscose sheet, in the presence of various amounts of sodium chloride. Transactions of the Faraday Society, 29(140), 1167–1180.

Nielsen LJ, Eyley S, Thielemans W, & Aylott JW (2010). Dual fluorescent labelling of cellulose nanocrystals for pH sensing. Chemical Communications, 46(47), 8929–8931. [PubMed: 21046033]

Ottesen V, Kumar V, Toivakka M, Chinga-Carrasco G, Syverud K and Gregersen ØW (2017). Viability and properties of roll-to-roll coating of cellulose nanofibrils on recycled paperboard. Nordic Pulp & Paper Research Journal, 32(2), 179–188.

Pei A, Butchosa N, Berglund LA, & Zhou Q (2013). Surface quaternized cellulose nanofibrils with high water absorbency and adsorption capacity for anionic dyes. Soft Matter, 9(6), 2047–2055.

Pérez S, & Mazeau K (2005). Conformations, structures, and morphologies of celluloses. Polysaccharides: Structural diversity and functional versatility, 41–68.

Purington E, Blakeley AR, Bousfield D, Gramlich WM (2017). Visualization of Latex and Starch in Paper Coatings by Tagging with Fluorescent Dyes. Nordic Pulp and Paper Research Journal, 32(03), 395–406.

Raj CR, Kamaraj M Emission of thioflavin T and its off-on control in polymer membranes. (2001). Photochemistry and Photobiology, 74(6), 752–759. [PubMed: 11783929]

Richmond F (2014). Cellulose nanofibers use in coated paper. The University of Maine.

Schut GR (1972): A study of different drying systems and the influence of their variables on the quality of coated papers. Wochenbl. Papierfabr 100:2,48.

Smith SA & Pretorius WA (2002). Spectrophotometric determination of pK$_a$ values for fluorescein using activity coefficient corrections. Water SA, 28(4), 395–402.

Wang S, Gao W, Chen K, Zeng J, Xu J, & Wang B (2018). An effective method for determining the retention and distribution of cellulose nanofibrils in paper handsheets by dye labeling. TAPPI JOURNAL, 17(3), 157–164.

Willis HF, Warwicker JO, Standing HA, & Urquhart AR (1945). The dyeing of cellulose with direct dyes. Part II. The absorption of chrysophenine by cellulose sheet. Transactions of the Faraday Society, 41, 506–541.

Wood PJ (1980). Specificity in the interaction of direct dyes with polysaccharides. Carbohydrate research, 85(2), 271–287.

Yang Q, & Pan X (2010). A facile approach for fabricating fluorescent cellulose. Journal of applied polymer science, 117(6), 3639–3644.

Zammarano M, Maupin PH, Sung LP, Gilman JW, McCarthy ED, Kim YS, & Fox DM (2011). Revealing the interface in polymer nanocomposites. ACS nano, 5(4), 3391–3399. [PubMed: 21410222]

Zang YH, Du J, Du Y, Wu Z, Cheng S, & Liu Y (2010). The migration of styrene butadiene latex during the drying of coating suspensions: when and how does migration of colloidal particles occur?. Langmuir, 26(23), 18331–18339. [PubMed: 21043465]

Zhang L, Li Q, Zhou J, & Zhang L (2012). Synthesis and Photophysical Behavior of Pyrene-Bearing Cellulose Nanocrystals for Fe3+ Sensing. Macromolecular Chemistry and Physics, 213(15), 1612–1617.

Zhou C, Wu Q, Lei T, & Negulescu II (2014). Adsorption kinetic and equilibrium studies for methylene blue dye by partially hydrolyzed polyacrylamide/cellulose nanocrystal nanocomposite hydrogels. Chemical Engineering Journal, 251, 17–24.
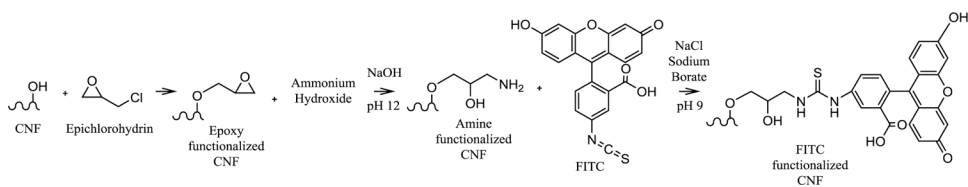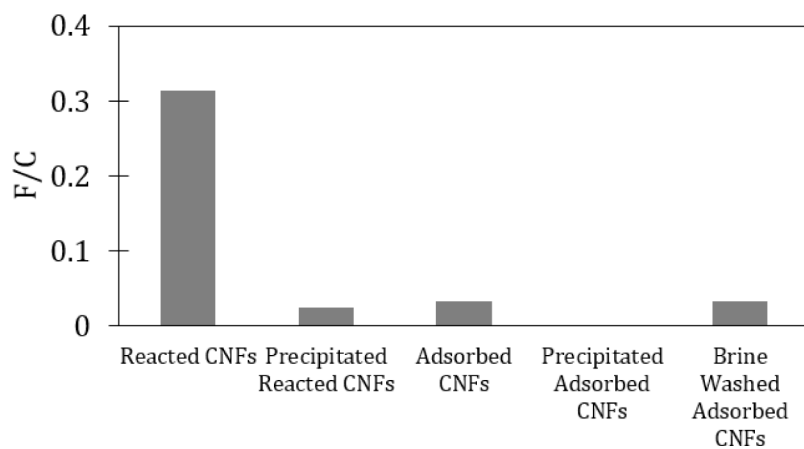
Figure 1:
Chemical reaction scheme for FITC functionalization of CNFs.

Figure 2:
Functionalization ratio as the mmol of FITC per mole of CNF glucose repeat unit (F/C) of FITC reacted CNFs, adsorbed FITC CNF, acetone precipitated FITC reacted CNFs, acetone precipitated adsorbed FITC CNFs, and brine washed adsorbed FITC CNFs.
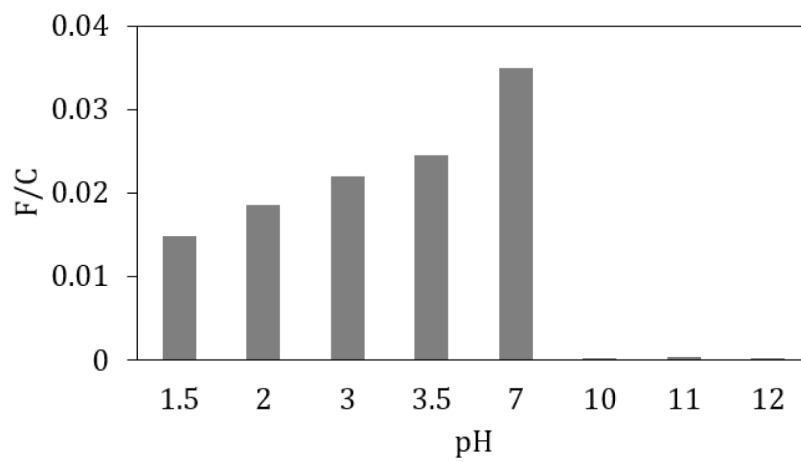
Figure 3:
Functionalization ratio (F/C) of pH treated adsorbed FITC CNFs post neutralization.
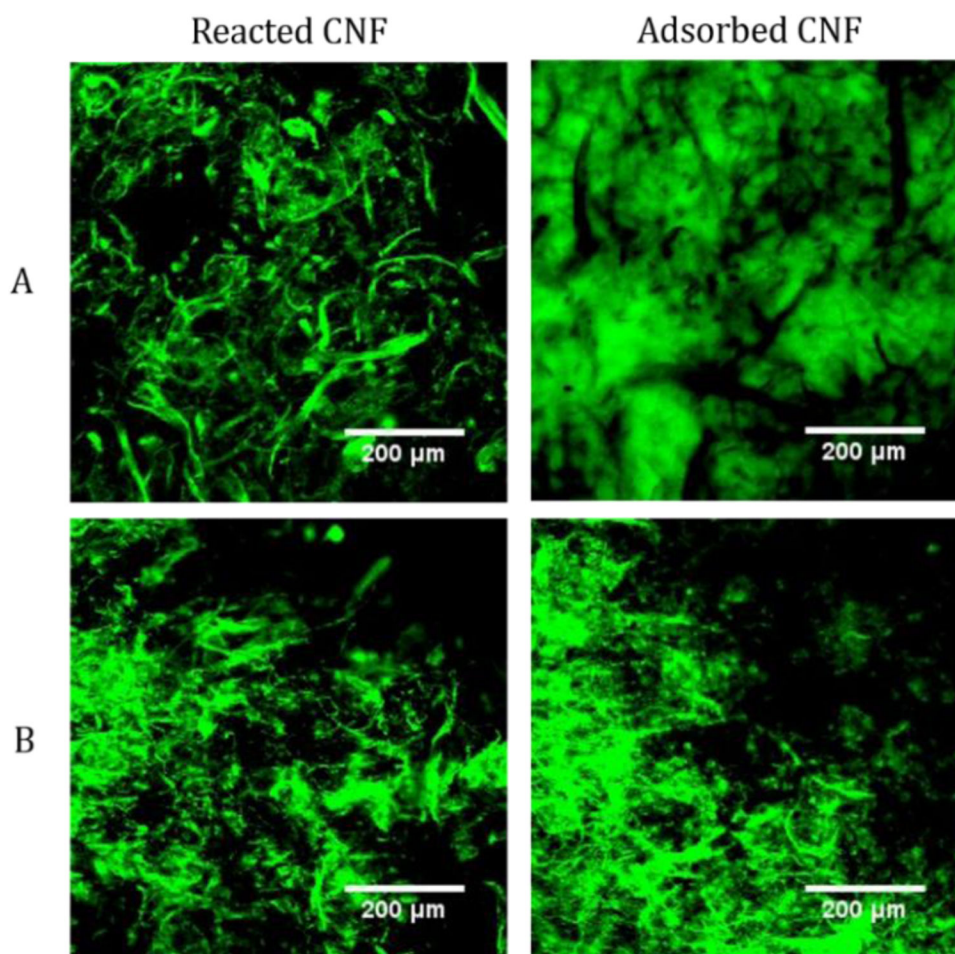
Figure 4:
Representative 2D CLSM images of wet (A) and dry (B) FITC reacted CNFs (left) and 1.5 pH treated FITC adsorbed CNFs (right).
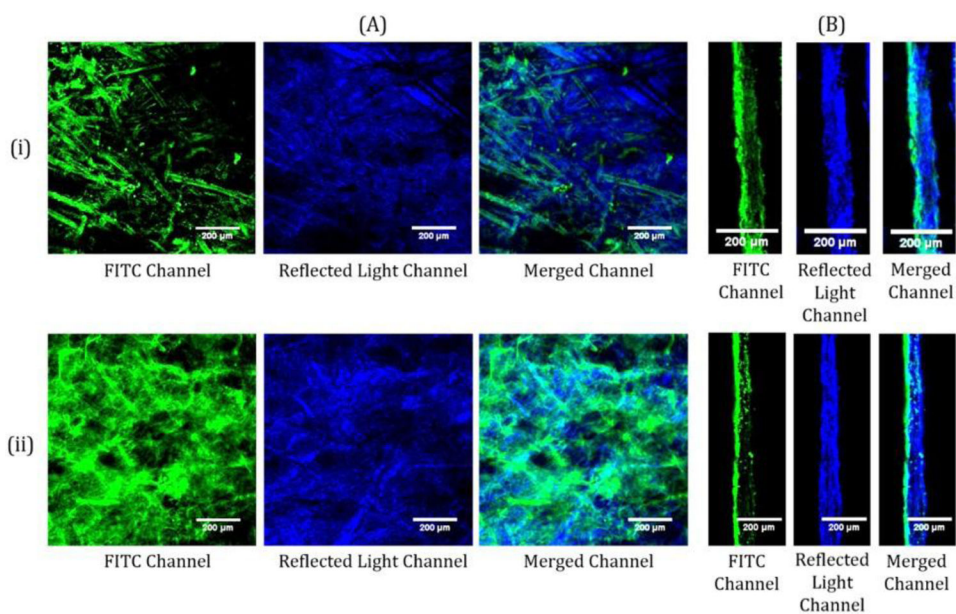
Figure 5:
Representative 2D (A) and cross section (B) CLSM images of adsorbed FITC CNFs (i) and FITC reacted CNFs (ii) on newsprint. The FITC channel shows the emissions from the FITC. The reflected light channel shows the light scattered at the surface of the paper. The merged channel combines the emissions and light scattering of the sample.
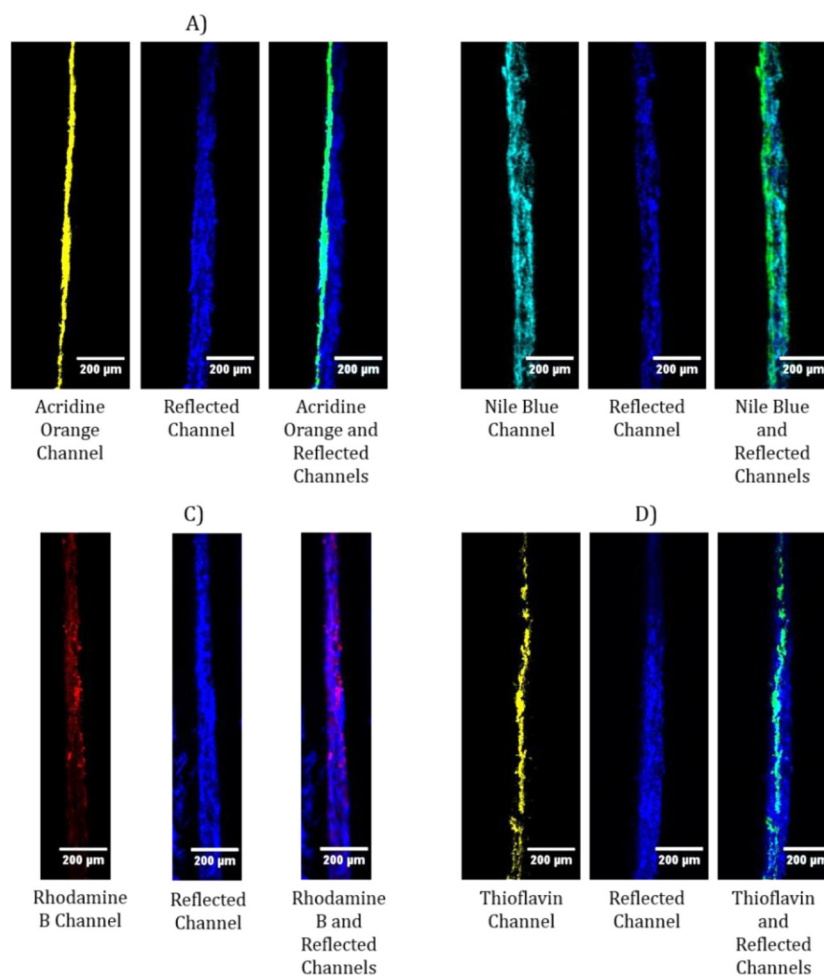
Figure 6:
Representative cross section CLSM images of adsorbed acridine orange (A), Nile blue (B), rhodamine b (C), and thioflavin (D) CNFs. CNFs were coated at 1.5% wt solids on newsprint with the coating on the left side of the paper.
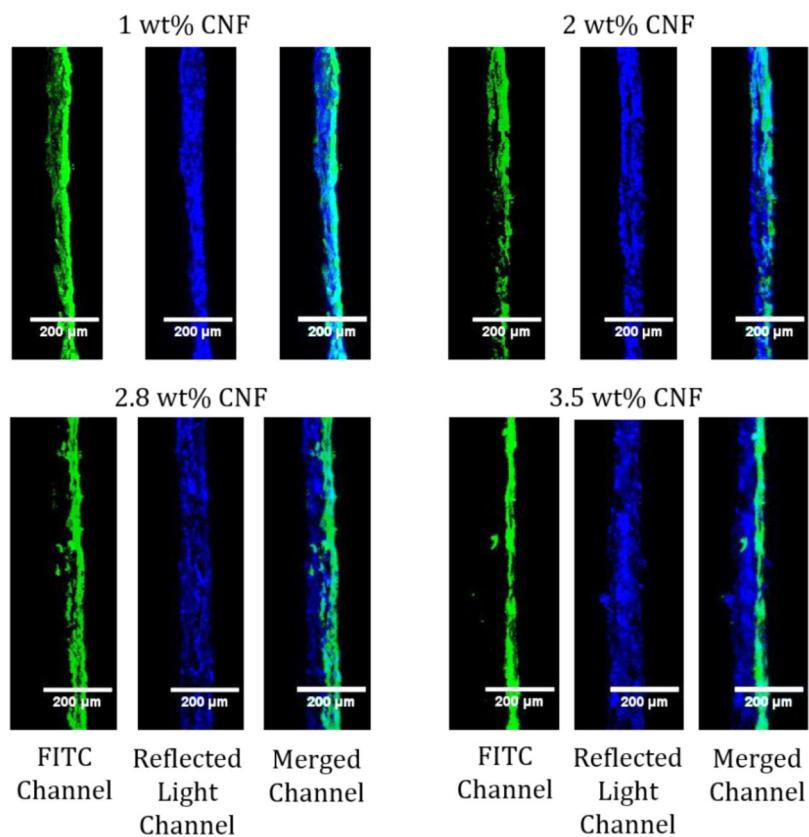
Figure 7:
Representative cross section CLSM images of 1, 2, 2.8, and 3.5 wt% CNF solids on newsprint with the coated surface on the right. The FITC channel shows the emissions from the FITC. The reflected light channel shows the light scattered at the surface of the paper. The merged channel combines the emissions and light scattering of the sample.

Table 1:

Excitation and emission acceptance wavelengths for the fluorescent dyes used.

Fluorescent Dye	Excitation Wavelength [nm]	Emission Acceptance Wavelength [nm]	Reflected Light Acceptance Wavelength [nm]
Acridine Orange	458	550 – 600	450 – 460
FITC	488	500 – 550	480 – 490
Nile Blue	633	720 – 800	630 – 640
Rhodamine B	543	600 – 650	540 – 550
Thioflavin	458	600 – 700	450 – 460
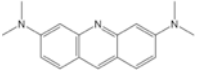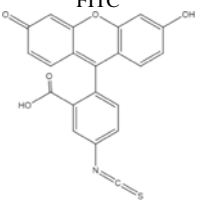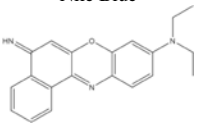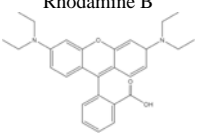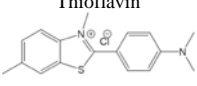
Table 2:

Chemical structures, molecular weights, topological polar surface areas (tPSAs), molecular charge at pH 7, and degree of functionalization of acridine orange, Nile blue, rhodamine B, and thioflavin dyed CNFs in terms of mmol of dye per mole of CNF repeat unit (F/C).

Dye	Molecular Weight [g/mol]	tPSA [Å²][a]	Charge at pH 7[b]	F/C
Acridine Orange	301.82	18.8	positive[c]	3.6
FITC	389.38	96.2	negative[d]	3.9×10^{-2}
Nile Blue	353.85	48.7	positive[e]	3.8×10^{-3}
Rhodamine B	479.02	53.0	zwitterion[f]	6.4×10^{-3}
Thioflavin	318.86	6.25	positives[g]	0.90

[a]Topological polar surface area as calculated by ChemDraw Prime v. 15.1

[b]Charge at pH 7 in water determined from pK_a values of proton exchangeable groups and literature.

[c]Murad 1999.

[d]Smith and Pretorius 2002.

[e]Ho 2006.

[f]Hinckley 1986.

[g]Raj and Ramaraj 2001.

Table 3:

Thickness of the paper and coating, and CNF signal depth determined from the CLSM images for 1.0,2.0, 2.8, and 3.5 wt% CNF solids on newsprint.

CNF Solids Content (wt%)	Paper and Coating Thickness [μm]	FITC Signal Depth [μm]	Percent Penetration in Paper [%]
1.0	53 ± 19	44 ± 17	84
2.0	54 ± 12	34 ± 14	80
2.8	85 ± 10	41 ± 10	20
3.5	89 ± 17	37 ± 8	9